

# Hyperfine structure of $\text{Tm}^{3+}$ in YAG for quantum storage applications

Ph. Goldner<sup>a,\*</sup>, O. Guillot-Noël<sup>a</sup>, A. Louchet<sup>b</sup>, F. de Sèze<sup>b</sup>, V. Crozatier<sup>b</sup>,  
I. Lorgeré<sup>b</sup>, F. Bretenaker<sup>b</sup>, J.L. Le Gouët<sup>b</sup>

<sup>a</sup> Laboratoire de Chimie Appliquée de l'Etat Solide, CNRS UMR 7574, ENSCP, 11 rue Pierre et Marie Curie, 75231 Paris Cedex 05, France

<sup>b</sup> Laboratoire Aimé Cotton, CNRS UPR 3321, Bâtiment 505, campus universitaire, 91405 Orsay Cedex, France

Available online 2 November 2005

## Abstract

Quantum storage of photons in an atomic ensemble can be obtained by using three-level  $\Lambda$  systems. In these schemes, two levels are coupled by optical transitions to a third one. Ideally, the two transitions should have similar intensities and long coherence lifetimes. Rare earth ion doped crystals are attractive materials for quantum storage because their hyperfine levels can have coherence lifetimes longer than 100  $\mu\text{s}$  and thus can be used to build  $\Lambda$  systems.  $\text{Tm}^{3+}$  ions are especially interesting since they can be excited by ultra-stable laser diodes. In this paper, the hyperfine structures of the  $^3\text{H}_6(0)$  and  $^3\text{H}_4(0)$  crystal field levels of  $\text{Tm}^{3+}$  in  $\text{Y}_3\text{Al}_5\text{O}_{12}$  are investigated by hole burning spectroscopy under a magnetic field. The results are compared to theoretical calculations and found to be in reasonable agreement. Moreover, it is shown that an appropriate magnetic field is able to relax the selection rule on the nuclear spin projection, an absolutely necessary condition to obtain an efficient three-level  $\Lambda$  system with  $\text{Tm}^{3+}$  in this host. Finally, a magnetic field orientation optimized with respect to the  $\Lambda$  system transition intensity ratio is predicted for a convenient experimental set-up.

© 2005 Elsevier B.V. All rights reserved.

## 1. Introduction

Quantum storage aims at transferring quantum states of photons into atomic ensembles. This is possible by using atomic species in which a three-level  $\Lambda$  system can be built [1]. The latter consists of two levels, which can both be coupled by light fields to a third one. The photon to be stored is resonant with one transition and a second light field with the other one. Intensity variation of the latter allows photons to be trapped and released [1]. To get an efficient trapping, the lifetimes of the coherences between the three levels of the  $\Lambda$  system, and especially between the two lower levels, have to be long. The optical transitions should also have similar intensities. Storage has been demonstrated for classical and quantum light in a number of systems [2–4]. Among these,  $\text{Pr}^{3+}:\text{Y}_2\text{SiO}_5$  has been shown to slow down and even stop light [5]. Rare earth doped crystals are attractive in quantum storage applications because their hyperfine levels can have long coherence lifetimes, like in

gases, with the added advantage of no atomic motion. However,  $\text{Pr}^{3+}$  ions optical transitions used in the three-level  $\Lambda$  system have to be excited by a dye laser which is very difficult to stabilize in the sub-kHz range. Alternatively,  $\text{Tm}^{3+}$  ions can be excited by laser diodes which can be very well stabilized [6]. The transition of interest takes place between the lowest crystal field (CF) level of the ground multiplet,  $^3\text{H}_6(0)$ , and the lowest CF level of an excited multiplet,  $^3\text{H}_4(0)$  around 793 nm. Under an external magnetic field, the hyperfine structure of these CF levels can be used to build a  $\Lambda$  system, as shown in Fig. 1. However, when the nuclear spin projections ( $M_I$ ) are good quantum numbers (as shown in Fig. 1), the 2–3 transition is forbidden since it would involve an optically driven spin flip. In previous works [7–9] on  $\text{Pr}^{3+}$  and  $\text{Tm}^{3+}$  ions, we have shown theoretically that an external magnetic field can induce very different nuclear spin projections by mixing ground and excited levels and thus relaxing the  $\Delta M_I = 0$  selection rule. In the case of  $\text{Tm}^{3+}$  in  $\text{Y}_3\text{Al}_5\text{O}_{12}$  (YAG) crystal, calculated branching ratio  $R$  between the 2–3 and 1–3 transitions can have values as high as 0.24 [7].

\* Corresponding author. Tel.: +33 1 44 27 67 07; fax: +33 1 46 34 74 89.  
E-mail address: [goldner@ext.jussieu.fr](mailto:goldner@ext.jussieu.fr) (Ph. Goldner).

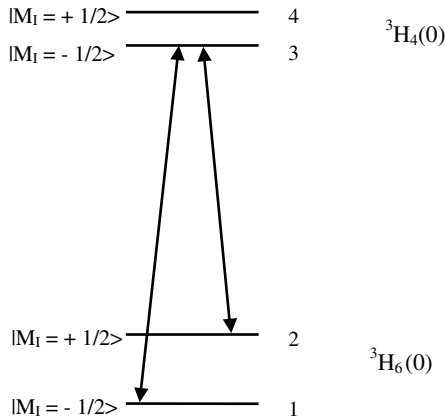


Fig. 1. A three-level  $A$  system in  $\text{Tm}^{3+}$  using the hyperfine levels of the  ${}^3\text{H}_6(0)$  and  ${}^3\text{H}_4(0)$  crystal field levels ( $I=1/2$ ). The arrows correspond to the optical transitions. If the nuclear spin projection is a good quantum number, the 2–3 transition is forbidden.

In this paper, we compare results obtained by hole burning spectroscopy with calculated hyperfine splittings and branching ratios. A reasonable agreement is found on hyperfine structures and breakdown of the nuclear spin projection selection rule is demonstrated under an appropriate magnetic field. The possibility of a high branching ratio in a convenient experimental set-up is also examined.

## 2. Theory

$\text{Tm}^{3+}$  is a non-Kramers' ion with 12 f electrons and a single natural isotope ( ${}^{169}\text{Tm}$ ) with a  $I=1/2$  nuclear spin. For symmetry sites which do not have at least one three-fold axis,  $\text{Tm}^{3+}$  electronic levels are singlets. In this case, no hyperfine structure appears without an external magnetic field [10]:  $\text{Tm}^{3+}$  electronic Hamiltonian commutes with the time reversal operator so there is no first-order hyperfine interaction. Moreover, due to the  $1/2$  value of the nuclear spin, magnetic quadrupole and second-order magnetic hyperfine interactions also vanish. This situation occurs for  $\text{Tm}^{3+}$  ions in YAG since they occupy  $D_2$  point symmetry sites. When an external magnetic field is applied, nuclear Zeeman and electronic Zeeman interactions combined with second-order hyperfine interaction lift the two-fold degeneracy of the nuclear spin projection. In the equivalent operator approximation, the hyperfine structure is simply given by the spin Hamiltonian [11]:

$$H_{\text{SH}} = \sum_{i=x,y,z} \gamma_i B_{0i} I_i \quad (1)$$

where  $\mathbf{B}_0$  is the magnetic field and  $\gamma_i$  the principal values of the effective enhanced nuclear gyromagnetic tensor. The principal axes of this gyromagnetic tensor coincide with the three two-fold axes of the  $D_2$  point symmetry group, denoted  $x$ ,  $y$ ,  $z$ . The gyromagnetic tensor depends on the CF level due to the electronic Zeeman and second-order hyperfine interactions:

$$\gamma_i = -g_n \beta_n - 2g\beta A_{ii}$$

with

$$A_{ii} = \sum_{n \neq 0} A \frac{|\langle 0 | J_i | n \rangle|^2}{E_n - E_0}$$

where  $g_n$  ( $g$ ) is the nuclear (electronic)  $g$ -factor and  $\beta_n$  ( $\beta$ ) the nuclear (electronic) Bohr magneton.  $A$  is the hyperfine constant and  $\mathbf{J}$  the total angular momentum. The index 0 denotes the first (lowest energy) CF level ( ${}^3\text{H}_6(0)$  or  ${}^3\text{H}_4(0)$ ),  $n$  the other CF-split levels of the considered multiplet and  $E_i$  is the energy of level  $i$ .

For magnetic fields non-collinear with the  $x$ ,  $y$  or  $z$  axis, the nuclear spin projection on any axis cannot be a good quantum number for all levels. As a result, the selection rule on the nuclear spin projection will no longer be generally true. This basic property shows that building a three-level  $A$  system may be possible in  $\text{Tm}^{3+}:\text{YAG}$ .

To see if that is the case for the  ${}^3\text{H}_6(0)$ – ${}^3\text{H}_4(0)$  transition, the hyperfine structure of  $\text{Tm}^{3+}$  in YAG has been theoretically determined from the diagonalization of its complete Hamiltonian for an arbitrary magnetic field orientation [7]. The latter includes free ion and crystal field Hamiltonians as well as electronic and nuclear Zeeman interactions and, finally, the hyperfine interaction. A spin Hamiltonian approximation has also been studied and has been found to reproduce well the results of the complete diagonalization. Calculations on the  ${}^3\text{H}_6(0)$  and  ${}^3\text{H}_4(0)$  levels show that the nuclear spin projection selection rules can be indeed relaxed for magnetic fields close to the local  $x$  axis. For a  $\mathbf{B}_0$  field in the  $x$ – $y$  plane and  $6^\circ$  away from the  $x$  axis,  $R=0.24$  and the wavefunctions of the 1, 2, 3 and 4 levels are

$$\begin{aligned} |1\rangle &= a|M_I = 1/2\rangle + b|M_I = -1/2\rangle \\ |2\rangle &= a|M_I = 1/2\rangle - b|M_I = -1/2\rangle \\ |3\rangle &= a'|M_I = 1/2\rangle + b'|M_I = -1/2\rangle \\ |4\rangle &= a'|M_I = 1/2\rangle - b'|M_I = -1/2\rangle \end{aligned}$$

with  $a = -0.2163 - 0.6732i$ ,  $b = 0.7071$ ,  $a' = -0.6665 - 0.2362i$ ,  $b' = 0.7071$ .

## 3. Experimental

Measurements were performed on a 5 mm thick 0.1%  $\text{Tm}^{3+}:\text{YAG}$  sample. The crystal was cut perpendicular to the  $[1\bar{1}0]$  axis. Hole burning spectra were obtained between 1.5 and 4.2 K using a stabilized laser diode operating at 793 nm and a 240 G magnetic field. The laser spot diameter on the sample was 800  $\mu\text{m}$ . The holes were burnt at center frequency in 10 shots of 50  $\mu\text{s}$  and the transition probed in 750  $\mu\text{s}$  over a 20 MHz interval. To ensure a nearly complete relaxation to the ground state after burning, the probe sequence was started 10 ms after the last burning pulse. This value was chosen to correspond to the lifetime of the intermediate  ${}^3\text{F}_4$  multiplet.

4. Results

4.1.  $Tm^{3+}$  sites in YAG

There are six identical sites for  $Tm^{3+}$  in YAG which are related to each other by cubic group symmetry operations. These sites have the same point symmetry,  $D_2$ , but are oriented in different directions, as shown in Fig. 2. The  $x, y, z$  local axes correspond to the three two-fold axes of the point symmetry group and are the principal axes of the gyromagnetic tensor.

However, even if the  $\gamma_i$  parameters are equal for all sites in the local frames, an external magnetic field will generally induce different hyperfine splittings for each site. For magnetic fields directed along some cubic symmetry axes, the number of inequivalent sites is reduced. For example, when

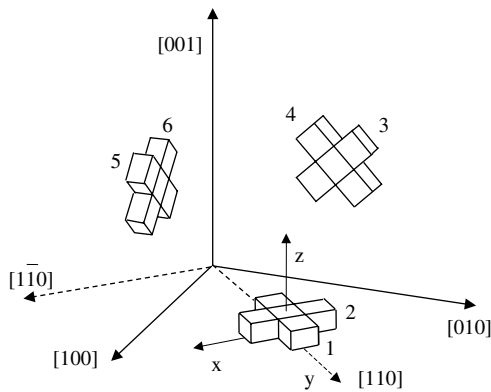


Fig. 2. Orientation of the six identical sites of  $Tm^{3+}$  in YAG with respect to the crystallographic axes. The local axes  $x, y, z$  correspond to the three two-fold axes of the  $D_2$  point symmetry. The crystal used in this work is cut perpendicular to the  $[1\bar{1}0]$  axis.

$B_0$  is along the  $[1\ 1\ 1]$  direction, sites 1, 3, 5 as well as sites 2, 4, 6 are equivalent.

For the  $^3H_4(0)-^3H_6(0)$  transition, the electric dipole moment is oriented along the  $y$  axis, according to Ref. [12]. This means that carefully chosen light polarization allows one to study a restricted number of sites. For example, when the light electric field is directed along the  $[1\ 1\ 0]$  direction, site 2 is not excited.

4.2. Hole burning experiments

When the laser shines on the sample at a given frequency, several classes of ions can absorb photons since the inhomogeneous linewidth of the  $^3H_4(0)-^3H_6(0)$  transition ( $\approx$ a few GHz) is much larger than typical hyperfine splittings ( $\approx$ 1–100 MHz). For a single  $Tm^{3+}$  site, Fig. 3 shows the four possible transitions between hyperfine levels which are resonant at a given burning frequency.

If the nuclear spin projection is a good quantum number, only two of these are allowed (thick lines). However, according to theoretical calculations, an appropriate magnetic field may relax the selection rules and the two forbidden transitions can be partially allowed (dotted thick lines). When the inhomogeneous line is probed after burning, a maximum of two holes and six anti-holes may appear besides the burned central hole at frequencies indicated in Fig. 3. The hole positions reflect the upper state splitting whereas the anti-holes are connected with upper and lower states splittings. Note that when the selection rules are valid, two anti-holes only can be observed since forbidden transitions cannot be excited in the burning step.

The efficiency of the holeburning process depends on the branching ratios between the excited hyperfine level and

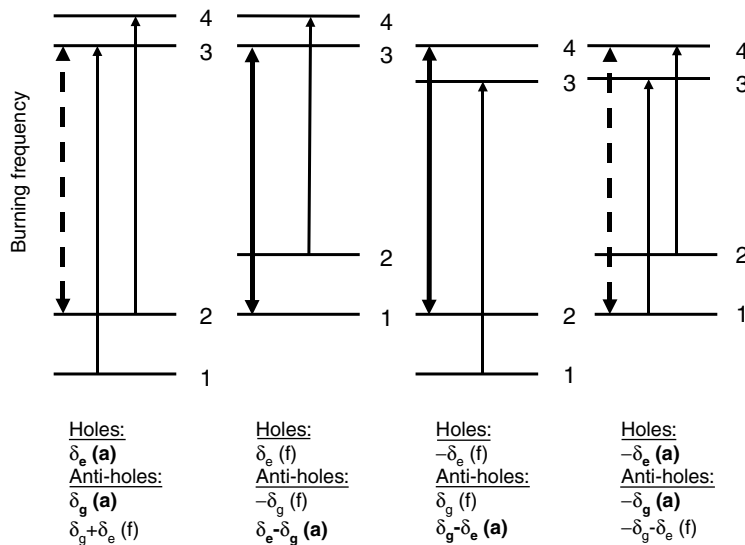


Fig. 3. Classes of ions resonant at a given burning frequency and resulting holeburning features for a single site in  $Tm^{3+}$ :YAG. The nuclear spin projection is assumed to be a good quantum number ( $B_0$  along one of the local axes  $x, y$  or  $z$ ): transitions 1–3, 2–4 are allowed and transitions 2–3, 1–4 are forbidden. Thick solid (dotted) lines: burning on allowed (forbidden) transitions. Thin solid lines: allowed transitions giving rise to side holes or anti-holes when probed. Below each scheme, the complete list of side structures is given with the energy difference from the burning frequency.  $\delta_e$  ( $\delta_g$ ) ground state (excited state) hyperfine splitting, (a) allowed, (f) forbidden.

the lower hyperfine ones. These are populated by several processes: thermal and flip–flop relaxations between the hyperfine levels, spontaneous emissions between the excited and ground states, and transitions (radiative and non-radiative) through the intermediate states  $^3H_5$  and  $^3F_4$ . Efficient burning is possible only if the pumping rate is higher than the relaxation rates, which tend to bring back the system to thermal equilibrium. However, if the relaxation rates are too low (typically at very low temperatures), the burning process becomes very efficient and even the probe may cause some burning. In this case, spectra become difficult to analyze and we slightly increased the temperature to about 4 K where the probe beam has no burning effect while holes and anti-holes are still clearly seen.

From the description of  $Tm^{3+}$  sites in YAG, it appears that the schemes of Fig. 3 have to be repeated for each site, leading to a very large number of burnt and probed transitions if the magnetic field direction and laser polarization are not well chosen. Although this may not be a problem in the building of a well defined three-level  $A$  system [7], complex spectra make determination of the gyromagnetic tensor and branching ratio between transitions difficult. For this reason, orientations of the magnetic field and laser polarization have been chosen to analyze only a few equivalent sites. Two examples are presented in the following.

#### 4.2.1. Magnetic field along the [111] direction

When the magnetic field is along the [111] direction, two classes of magnetically equivalent sites (1, 3, 5 and 2, 4, 6) appear. Moreover, by polarizing the laser along the [111] direction too, only sites 1, 3, 5 are excited since the electric field has no  $y$ -component for sites 2, 4, 6. The corresponding hole burning spectrum is shown in Fig. 4. The zero frequency hole as well as two anti-holes at  $6.27 \pm 0.03$  MHz from the central peak are observed. As discussed above, this spectrum corresponds to the excitation and subsequent probing of allowed transitions only (see Fig. 3). The anti-holes are then located at  $\pm(\delta_g - \delta_e)$ , where  $\delta_g$  ( $\delta_e$ ) is the ground (excited) state hyperfine splitting. For this magnetic field orientation and magnitude, the theoretical value for

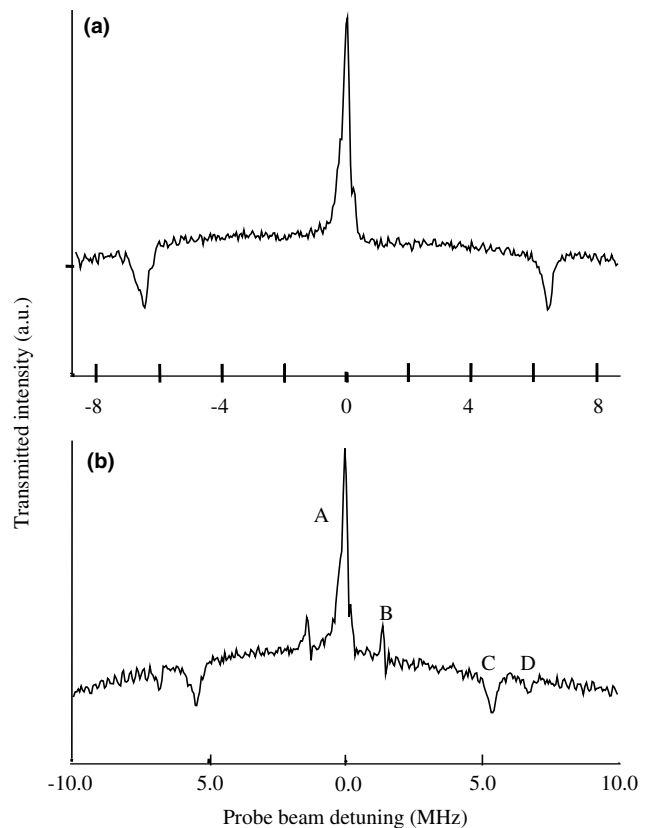


Fig. 4. Hole burning spectrum obtained with the magnetic field and the laser polarization along the [111] (a) and [001] (b) directions. ( $B_0 = 240$  G). A: central hole, B: hole, C, D: anti-holes.

( $\delta_g - \delta_e$ ) is 9.42 MHz (see Table 1) is in a reasonable agreement with experiment. The calculated branching ratio between the 2–3 and 1–3 transitions is very small ( $5 \times 10^{-4}$ ) which corresponds well to burning and probing on allowed transitions only.

#### 4.2.2. Magnetic field along the [001] direction

In this configuration, the sites are also divided into two groups: 1, 2 and 3, 4, 5, 6. Laser polarization is also fixed

Table 1

Calculated hyperfine splittings of the  $^3H_6(0)$  ( $\delta_g$ ) and the  $^3H_4(0)$  ( $\delta_e$ ) crystal field levels under several  $B_0$  magnetic field orientations for the six sites of  $Tm^{3+}$  in YAG

Site number	$\delta_g$ (MHz)	$\delta_e$ (MHz)	$\delta_g - \delta_e$ (MHz)	$R$
$B_0$ along [111]				
1,3,5	10.83	1.41	9.42 ( <b>6.27</b> )	0.0005
2,4,6	0.40	0.42		0.0099
$B_0$ along [001]				
1,2	0.27	0.15		0
3,4,5,6	9.38 ( <b>6.85</b> )	1.27 ( <b>1.43</b> )	8.11 ( <b>5.41</b> )	0.0159
$B_0$ in the ([001], [110]) plane and $49^\circ$ away from [001]				
1	10.01	1.31		0.0008
2	0.39	0.39		0.0137
3,5	11.15	1.45		0.0006
4,6	1.22	0.48		0.2354

Experimental values (precision  $\pm 0.03$  MHz) are given in bold characters inside brackets. The field amplitude is 240 G. The  $R$  parameter is the branching ratio between the 2–3 and 1–3 transitions (see Fig. 1).

along the [001] axis and therefore only sites 3, 4, 5 and 6 are excited. The holeburning spectrum (Fig. 4) presents two holes and four anti-holes in addition to the central hole. This can be understood with Fig. 3 schemes if burning is allowed on all transitions. Probing should reveal two extra anti-holes at  $\pm(\delta_g + \delta_e)$  but since the probing intensity is much lower than that of the burning pulse, the corresponding forbidden transitions are probably too weak to be observed. According to Fig. 3, the side holes are located at  $\pm\delta_e$  from the central line and the anti-holes at  $\pm\delta_g$  and  $\pm(\delta_g - \delta_e)$ , giving  $\delta_e = 1.43 \pm 0.03$  MHz and  $\delta_g = 6.85 \pm 0.03$  MHz. In this case too, the observed splittings are in reasonable agreement with theoretical values for  $\delta_g$  and in very good agreement for  $\delta_e$  (Table 1). The calculated branching ratio also explains that burning is possible on the forbidden transitions (it is 30 times higher than in the previous experiment). However, probing these forbidden transitions at low power is still very difficult ( $R = 0.0159$ ).

## 5. Discussion

In the previous section, experimental and calculated values are found to agree within approximately 50% in the worst case. This result can also be described in terms of the gyromagnetic tensor. In the spin Hamiltonian approximation, the hyperfine splitting of crystal field levels is given by

$$\delta = \sqrt{\gamma_x^2 B_{0x}^2 + \gamma_y^2 B_{0y}^2 + \gamma_z^2 B_{0z}^2} \quad (2)$$

Taking into account the magnetic field orientation with respect to the local axes for each excited site, the measured values of  $\delta_e$  and  $\delta_g$  are related to the gyromagnetic tensor by

$$\frac{B_0}{\sqrt{2}} [\gamma_{x,g}^2 + \gamma_{y,g}^2]^{1/2} = 6.85 \pm 0.03 \text{ MHz} \quad (3)$$

for the ground state and

$$\frac{B_0}{\sqrt{2}} [\gamma_{x,e}^2 + \gamma_{y,e}^2]^{1/2} = 1.43 \pm 0.03 \text{ MHz} \quad (4)$$

for the excited state. The experiment with  $\mathbf{B}_0$  along the [111] axis also gives

$$\frac{B_0}{\sqrt{3}} [2(\gamma_{y,g}^2 - \gamma_{y,e}^2) + \gamma_{z,g}^2 - \gamma_{z,e}^2]^{1/2} = 6.27 \pm 0.03 \text{ MHz} \quad (5)$$

Theoretical calculations show that  $\gamma_y^2 \gg \gamma_x^2, \gamma_z^2$  for both the ground and excited states. This is completely consistent with Eqs. (3)–(5) and gives  $\gamma_{y,g} = 403$  MHz/T and  $\gamma_{y,e} = 82$  MHz/T. Those values also agree quite well with calculations:  $\gamma_{y,g,\text{cal}} = 560$  MHz/T and  $\gamma_{y,e,\text{cal}} = 75$  MHz/T. The larger discrepancy in the ground state values may be related to the accuracy of some calculated crystal field wavefunctions of the  $^3\text{H}_6$  multiplet.

An important point is that the fundamental property of the system, i.e. the large variation between ground and

excited state  $\gamma_y$  values, is reproduced by the calculations. This suggests that selection rules on nuclear spin projections can be actually released with appropriate magnetic fields. The predicted strong anisotropy of the gyromagnetic tensor, which is mainly directed along the  $y$  axis, also seems to be experimentally observed. Further experiments are under way to completely determine the ground and excited state gyromagnetic tensors.

Since our sample is cut perpendicular to the  $[1\bar{1}0]$  axis, it would be experimentally very convenient to find a magnetic field orientation in the  $([001], [110])$  plane which would optimize the branching ratio between 2–3 and 1–3 transitions for some sites. These transitions would also have to be excited by a laser propagating along the  $[1\bar{1}0]$  axis. Since calculated hyperfine splittings seem reasonable, we have computed the branching ratio  $R$  between 2–3 and 1–3 transitions as a function of  $\mathbf{B}_0$  orientation in the  $([001], [110])$  plane for a laser polarized along the  $[111]$  direction. In this case, sites 1, 3, 5 are not excited and sites 4 and 6 are magnetically equivalent.

The corresponding curve is shown on Fig. 5. It is worth noting that around the [111] direction, large values of  $R$  are expected. They are very close to the maximum value (0.24) which can be obtained in the system [7]. Hyperfine splittings corresponding to the magnetic field  $\mathbf{B}_0$  directed  $49^\circ$  away from the [001] axis, i.e. to a position of maximum branching ratio, are reported in Table 1. These values are obtained at a 240 G field. In order to get larger splittings, a stronger magnetic field (4500 G) will be used. This will have no effect on the branching ratios. Under these conditions, it should be possible to build a three-level  $\Lambda$  system with the sample studied here by using the protocol described in Ref. [7]. This experimental configuration has also the advantage of using two equivalent sites, which increases the absorption coefficient compared to schemes

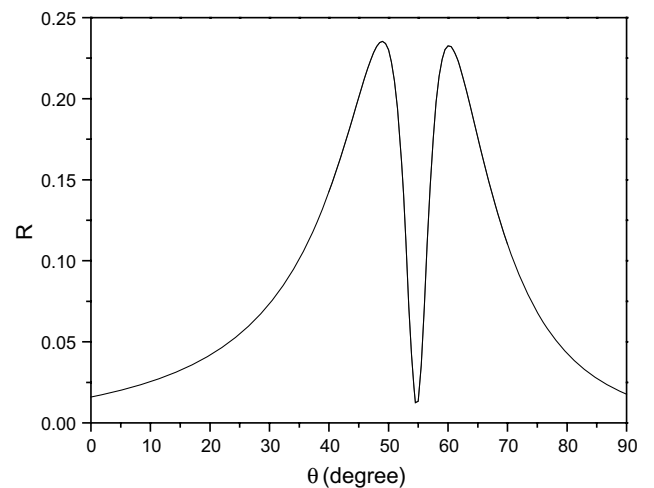


Fig. 5. Branching ratio  $R$ , for sites 4 and 6, between the 2–3 and 1–3 transitions as a function of the angle  $\theta$  between the magnetic field and the [001] axis. The magnetic field is kept in the  $([001], [110])$  plane. For  $\mathbf{B}_0$  along the  $[111]$  direction ( $\theta = 54.5^\circ$ ),  $R$  is minimal.

were only one site is excited. This is important since quantum storage requires high absorption coefficients.

## 6. Conclusion

Hole burning experiments have been performed in  $\text{Tm}^{3+}:\text{YAG}$  on the  ${}^3\text{H}_6(0) \rightarrow {}^3\text{H}_4(0)$  transition at low temperature and under a magnetic field. Holes and anti-holes have been observed for two magnetic field orientations and laser polarizations chosen to decrease the number of optically excited and magnetically non-equivalent sites. Comparison with calculated hyperfine splittings from crystal field wavefunctions shows a reasonable agreement. Analysis of the results in terms of the gyromagnetic tensor suggests that the wavefunctions are strongly anisotropic in ground and excited states, also in agreement with theoretical predictions. The estimated values of  $\gamma_y$  are significantly different in the ground and excited states, which is very favourable for relaxation of the selection rules for the 2–3 transition. Finally, an optimized orientation of the magnetic field with respect to the 2–3 to 1–3 transitions branching ratio has been calculated in the  $([001], [110])$  plane. This configuration has the advantage of a simple experimental set-up as well as a large absorption coefficient which is necessary for quantum storage.

## Acknowledgement

This work is partially supported by the European project ESQUIRE IST-2001-38871.

## References

- [1] M.D. Lukin, *Rev. Mod. Phys.* 75 (2003) 457.
- [2] M.S. Bigelow, N.N. Lepeshkin, R.W. Boyd, *Phys. Rev. Lett.* 90 (2003) 113903.
- [3] B. Julsgaard, J. Sherson, J.I. Cirac, J. Fiurasek, E.S. Polzik, *Nature* 432 (2004) 482.
- [4] D.F. Phillips, A. Fleischhauer, A. Mair, R.L. Walsworth, M.D. Lukin, *Phys. Rev. Lett.* 86 (2001) 783.
- [5] A.V. Turukhin, V.S. Sudarshanam, M.S. Shahriar, J.A. Musser, B.S. Ham, P.R. Hemmer, *Phys. Rev. Lett.* 88 (2002) 023602.
- [6] V. Crozatier, F. de Sèze, L. Haals, F. Bretenaker, I. Lorgère, J.-L. Le Gouët, *Opt. Comm.* 241 (2004) 203.
- [7] O. Guillot-Noël, Ph. Goldner, E. Antic-Fidancev, J.L. Le Gouët, *Phys. Rev. B* 71 (2005) 174409.
- [8] Ph. Goldner, O. Guillot-Noël, *Mol. Phys.* 102 (2004) 1185.
- [9] Ph. Goldner, O. Guillot-Noël, *Opt. Mater.* 28 (2006) 21.
- [10] A. Abragam, B. Bleaney, *Electron Paramagnetic Resonance of Transition Ions*, Dover Publications Inc., New York, 1986.
- [11] R.M. Macfarlane, R.M. Shelby, in: A.A. Kaplyanskii, R.M. Macfarlane (Eds.), *Spectroscopy of Solids Containing Rare Earth Ions*, North-Holland, Amsterdam, 1987, p. 51.
- [12] Y. Sun, G.M. Wang, R.L. Cone, R.W. Equall, M.J.M. Leask, *Phys. Rev. B* 62 (2000) 15443.